

Elisabeth John, Jan Dirk Epping, Dietmar Stephan

## The influence of the chemical and physical properties of C-S-H seeds on their potential to accelerate cement hydration

Open Access via institutional repository of Technische Universität Berlin

### Document type

Journal article | Accepted version

(i. e. final author-created version that incorporates referee comments and is the version accepted for publication; also known as: Author's Accepted Manuscript (AAM), Final Draft, Postprint)


### This version is available at

<https://doi.org/10.14279/depositonce-15353>

### Citation details

John, E., Epping, J. D., & Stephan, D. (2019). The influence of the chemical and physical properties of C-S-H seeds on their potential to accelerate cement hydration. In *Construction and Building Materials* (Vol. 228, p. 116723). Elsevier BV. <https://doi.org/10.1016/j.conbuildmat.2019.116723>.

### Terms of use

 This work is licensed under a Creative Commons Attribution-NonCommercial- NoDerivatives 4.0 International license: <https://creativecommons.org/licenses/by-nc-nd/4.0/>

# 1 The influence of the chemical and physical 2 properties of C-S-H seeds on their potential to 3 accelerate cement hydration

4 Elisabeth John<sup>a</sup>, Jan Dirk Epping<sup>b</sup>, Dietmar Stephan<sup>a\*</sup>

5 <sup>a</sup> Institute for building materials and construction chemistry, TU Berlin, Gustav-Meyer-Allee 25, 13355  
6 Berlin

7 <sup>b</sup> Institute of chemistry, TU Berlin, Straße des 17. Juni, 10623 Berlin

8 \* Corresponding author (stephan@tu-berlin.de)

## 9 1. Abstract

10 The development of green cements and reduced cement contents in concrete for reducing CO<sub>2</sub>  
11 emissions, often results in reduced hydration activity and strength, especially in early stages, which  
12 conflicts with economic interests and process requirements.

13 Besides pozzolans like nano-silica, the performance of calcium silicate hydrate (C-S-H)  
14 nanoparticles has recently become a focus of research, due to their outstanding ability to accelerate  
15 cement hydration, without compromising the long-term strength of the seeded cement. Many C-S-H  
16 properties have been found to influence their accelerating performance, with controversial results having  
17 been published regarding the calcium to silicon ratio. While Alizadeh et al. have found that the hydration  
18 of C<sub>3</sub>S is accelerated more when C-S-H seeds richer in silicon are applied, Land et al. have found that  
19 seeds richer in calcium are better accelerators. Neither particle size nor respective surface area were kept  
20 constant in either work.

21 Using stoichiometry within the stability range of C-S-H, this work aims towards a systematic  
22 investigation of the influence of the chemical and physical properties of C-S-H. The impact on cement  
23 hydration is examined using isothermal heat flow calorimetry as a screening method.



25

26 **Keywords:** C-S-H seeding; cement hydration; calcium to silicon ratio

27 **3. Introduction**

28 Calcium silicate hydrate (C-S-H<sup>1</sup>) is the major hydration product of Portland cement based concrete,  
 29 the most widely used material on the planet [1,2]. Although cement-based materials have been used for  
 30 more than a century and have been researched intensively for decades, the detailed molecular

---

<sup>1</sup> Construction chemistry nomenclature: C = CaO, S = SiO<sub>2</sub>, H = H<sub>2</sub>O

31 mechanisms of cement hydration have not been fully resolved yet, with the exact crystallography of C-  
32 S-H also remaining unclear.

33 Early investigations towards the structure of C-S-H proposed a distorted mix of jennite ( $C/S = 1.5$ )  
34 and  $14\text{\AA}$  tobermorite-like ( $C/S = 0.83$ ) layers, with the structure of jennite itself remaining unresolved  
35 until 2004 [3,4]. Both, tobermorite and jennite feature a layered structure of quasi indefinite silicate  
36 chains intermitting with Ca-O sheets. While in the main calcium layer of tobermorite only Ca-O bonds  
37 are present, in contrast jennite also contains Ca-OH bonds. The interlayer spaces of both structures are  
38 characterized by water molecules and calcium ions. Another model describes C-S-H in terms of a  
39 defective tobermorite structure, mixed with calcium hydroxide, which might either be present in the  
40 interlayer spaces or as a discrete phase at a higher  $C/S$  [5]. It was recently found that C-S-H has a  
41 tobermorite-like structure, even at higher  $C/S$  ratios, giving support to the calcium hydroxide theory [6].

42 Promising investigations have shown that the addition of small quantities of synthetic C-S-H to  $C_3S$   
43 or cement pastes, can significantly accelerate the hydration rate and strength development of  
44 cementitious materials [7,8]. The acceleration is attributable to nucleation seeding, with the product  
45 formation having been shown to shift away from the clinker surfaces, towards the dispersed synthetic  
46 C-S-H in the pore space [9,10]. Not only did this phenomenon reduce the thickness of the hydration  
47 product layers around the clinker, but it has been proposed that it induces a concentration gradient of  
48  $Si^{4+}$ ,  $OH^-$  and  $Ca^{2+}$  ions from clinker to seed [11].

49 The particle size of the seeding material has unanimously been found to impact on acceleration  
50 performance. The preparation of calcium silicate hydrates in the presence of polymers, usually  
51 polycarboxylate ethers, is able to successfully stabilize C-S-H nano-particles [12]. The interaction of  
52 organic molecules with calcium silicate hydrates has been a subject of research for many years, since  
53 additives like accelerators, retarders, liquefiers and other organic regulators make up an essential part of  
54 modern high-performance concretes. It appears that the interaction of C-S-H with organic molecules is  
55 rather complex, with weak electrostatic interactions and hydrogen bridging having been reported, as  
56 well as the intercalation of small molecules into the C-S-H interlayer spaces and the covalent grafting  
57 of polymers on the defect sites of the silicate structure [13–16]. Besides the physical particle properties,  
58 the calcium to silicon ratio of C-S-H has been observed to alter the resulting acceleration, with

59 contradictory results having been published by Alizadeh et al. and Land et al. Whilst in the latter work  
60 it was observed that a high C/S ratio leads to stronger acceleration in cement, Alizadeh et al. have  
61 reported better performance of seeds with a lower C/S in C<sub>3</sub>S [11,17,18]. Other authors have not been  
62 able to induce any significant changes through the manipulation of the calcium to silicon ratio [10].

63 Practical interests, as well as academic ones, would benefit if the role of synthetic C-S-H in cement  
64 hydration was understood. The assumption that synthetic C-S-H intervenes in the nucleation and growth  
65 of hydration products, might help in understanding the complex reaction system of dissolution and  
66 precipitation, during cement hydration, in more detail. From a practical point of view, the generation of  
67 performance-property relationships will allow a tailored synthesis of C-S-H seeds, which will make it  
68 possible to avoid the unwanted side effects of many conventional accelerators,, like enhanced  
69 corrosiveness or compromised long-term compressive strength [11,19,20]. Additionally, calcium  
70 silicate hydrates can be produced with high cost efficiency from cheap and nontoxic starting materials  
71 [18,21,22].

72 The aim of the current study is to investigate the impact of the calcium to silicon ratio of C-S-H  
73 seeds, on their performance as additives in cementitious materials and to correlate these findings with  
74 the properties of the hydrate. Although polymer stabilized C-S-H is known to show good performance  
75 and a long shelf life, a polymer-free synthesis was chosen in the current investigation so as to avoid the  
76 superimposition of effects.

#### 77 **4. Experimental section**

##### 78 *Materials*

79 C-S-H was prepared from freshly calcined calcium oxide, demineralized water and a colloidal silicon  
80 dioxide dispersion (Köstrosol 0730, *CWK*). The cement was supplied by *CEMEX* (CEM I 42.5 R and  
81 CEM I 52.5 R) and *Optera* (CEM I 52.5R). Triclinic C<sub>3</sub>S was prepared by the VUSTAH research  
82 institute for building materials in Brno, Czech Republic.

##### 83 *Synthesis and sample preparation*

84 Semi-crystalline C-S-H was prepared by the pozzolanic reaction of CaO, SiO<sub>2</sub> and water in a calcium  
85 to silicon ratio of 0.7 or 0.8, 1.0 and 1.2. The higher C/S ratio of 0.8 was chosen for the low-lime C-S-  
86 H as the investigation advanced, since 0.7 represents the lower limit of the stability of the system. A  
87 slightly higher ratio of 0.8 prevents by-product formation. For the pozzolanic synthesis, the starting  
88 materials were mixed to the desired calcium to silicon (C/S) and water to solid ratios (w/s), after which  
89 the suspension was transferred into plastic bottles and kept under constant mixing in a shaker for 24h,  
90 unless stated otherwise (at ambient conditions); alternatively, they were transferred to a planetary ball  
91 mill (Pulverisette 5, *Fritsch*). The milling procedure included break intervals, so as to avoid heating the  
92 suspension, with an effective milling time of 12 hours being applied.

93 For characterization, the C-S-H was dried in a vacuum, with hydrating C<sub>3</sub>S samples stopped by  
94 solvent exchange with isopropanol and dried at 40°C.

95 For application, C-S-H was primarily suspended as prepared in water for 1 minute, with an ultrasonic  
96 rod. The water to binder ratio was 0.5, unless stated otherwise.

### 97 *Characterization*

98 The **mineralogy** of the samples was investigated with x-ray diffraction (PANalytical Empyrian,  
99 PIXcel 1D Detector, Cu K<sub>α</sub>, *Panalytical*), while the **silicate polymerization** of pure C-S-H and the C<sub>3</sub>S  
100 specimens was analysed with <sup>29</sup>Si-MAS-NMR (Avance 400, 400 MHz, *Bruker*). **Thermogravimetric**  
101 **analysis** was performed under a nitrogen atmosphere, in a temperature range of 25 to 950 °C, with a heating  
102 rate of 10 K/min (TG 209 Tarsus F3, *Netzsch*). The **specific surface area** was determined through cryogenic  
103 nitrogen adsorption (Sorptomatic 1900, *Carlo Erba Instruments*, BET). **Particle size** analysis was  
104 carried out in water (Mastersizer 2000, *Malvern Instruments*), with the C-S-H suspension being  
105 dispersed with an ultrasonic rod for one minute, before measuring. A reflective index of 1.68 for C-S-H  
106 and 1.33 for water was used for the calculations. **Calorimetry** data was obtained from externally mixed  
107 pastes containing 10g cement and 5g water, in at least a three-fold determination, with the average being  
108 shown. The C-S-H was suspended for 1 minute in water with an ultrasonic rod. Data points were  
109 recorded every 10s at 20°C (Isothermal heat flow calorimeter MC-CAL100, *C3 Analysentechnik*).  
110 **Compressive strength** tests were conducted on 20mm<sup>3</sup> cubes (Type 2060, *TONI Technik GmbH*) and

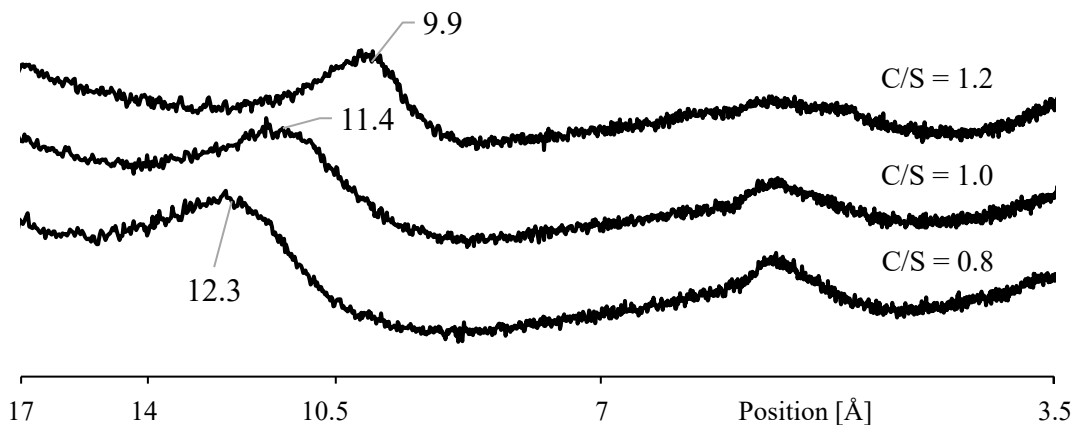
111 the results were calculated as an average from 6 measurements each. C-S-H was applied as described  
 112 for calorimetry investigations. The characterization of the setting behaviour was done by **Vicat needle**  
 113 **penetration** testing, according to EN 196-3, with an automatic Vicat device (ToniSET, *Toni Technik*).  
 114 The setting and hardening performance of the pastes was additionally monitored by **ultrasonic sound**  
 115 **speed measurements** (IP-8, *Ultratest*). **Rheological** investigations were conducted with the pastes  
 116 prepared as for calorimetry investigations, with the basket geometry of the viscomat NT (*Schleibinger*  
 117 *Geräte*) being used in the experiment . The rotation speed was increased from 0 to 150 rpm in 5 steps  
 118 of 30 rpm. Each step was kept at a constant speed for 60 seconds, with the 150 rpm plateau being kept  
 119 constant for 180 s. After reaching the maximum, the speed was lowered back to zero in the same  
 120 stepwise manner. Plastic viscosity ( $\eta$ ) and yield stress ( $\tau_0$ ) were calculated with at least 20 constant  
 121 values at the end of each step, according to the Bingham equation (1).

$$122 \quad \tau = \tau_0 + \eta(\dot{\gamma}) \quad (1)$$

## 123 5. Results and Discussion

### 124 5.1. Characterization of the calcium silicate hydrates

125 The mineralogical properties of C-S-H were investigated by XRD and  $^{29}\text{Si}$  MAS-NMR. The typical  
 126 broad X-ray reflexes, with the main peak at around  $29^\circ 2\theta$ , reflect the distorted structure of C-S-H and  
 127 the small dimension of coherent diffractive regions [23].



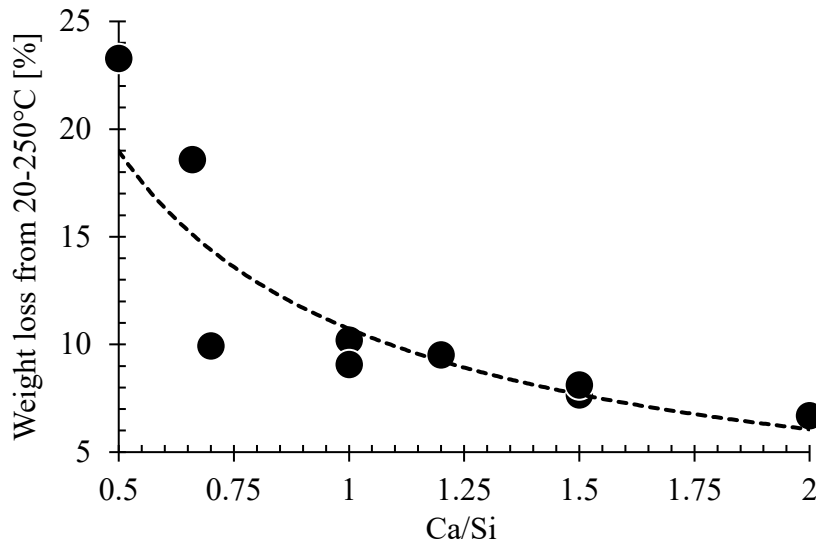
128

129 *Fig. 1: X-ray diffractogram of C-S-H prepared with different calcium to silicon ratios. The basal spacing decreased with rising calcium*

130

*levels, from 12.3 to 9.9Å. The intensity of the 5Å reflex was enhanced with the silicon content.*

131 Differences in diffraction, depending on the stoichiometry used, can be observed in the small angle  
 132 region shown in Fig. 1. The basal 001 reflex, at approximately 10 Å, shifted to higher angles when the  
 133 calcium level increased. Additionally, the reflex intensity at approximately 5 Å decreased. The  
 134 decreasing basal spacing can be mainly attributed to the quantity of water present in the interlayers,  
 135 which decreased with C/S (Fig. 2). Because the water content of C-S-H is sensitive to the drying method  
 136 applied, the samples were all vacuum-dried for comparability. Since the water content was determined  
 137 by thermogravimetric analysis, discrimination between pore and crystal water was not possible. In solid-  
 138 state <sup>29</sup>Si NMR two peaks were found, referring to end chain silicate units (Q<sup>1</sup>, -78 to -84 ppm) and inner  
 139 chain silicate units (Q<sup>2</sup>, -84 to -90 ppm) respectively. No signals referring to unreacted silica (Q<sup>4</sup>), or  
 140 other silicate species with a higher degree of polymerization than Q<sup>2</sup>, were found (Fig. 3).

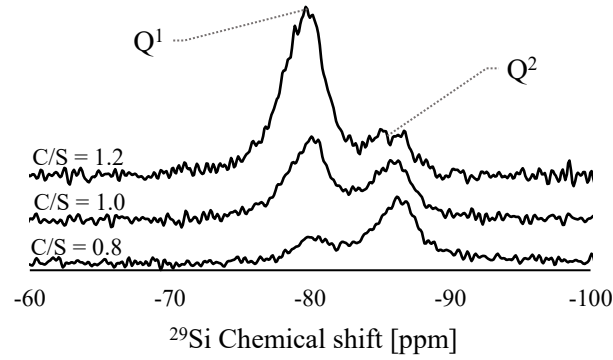


141  
 142 *Fig. 2: Weight loss attributed to crystal and pore water from C-S-H, in relation to the calcium to silicon ratio. The specimens for TG*  
 143 *analysis were dried in a vacuum*

144 It was found that, with a decreasing calcium to silicon ratio the degree of silicate polymerization was  
 145 enhanced, so that C<sub>0.8n</sub>S<sub>n</sub>H<sub>x</sub> (C/S = 0.8) had a silicate chain length of approximately 10, while C<sub>1.2n</sub>S<sub>n</sub>H<sub>x</sub>  
 146 (C/S = 1.2) was mostly dimeric. The mean chain length ( $\overline{CL}$ ) was calculated from the Q<sup>1</sup> to Q<sup>2</sup> ratio,  
 147 according to equation 2. The gradual depolymerization of the wollastonite-like silicate chains, through  
 148 the absence of bridging silicates, was reflected in the decreasing 5 Å reflex in XRD.

149 
$$\overline{CL} = \frac{2 \cdot (Q^1 + Q^2)}{Q^1} \quad (2)$$





150

151

152

*Fig. 3: Silicate polymerization, depending on the calcium to silicon ratio. The ratio of  $Q^2:Q^1$  and consequently the mean silicate chain length, calculated according to equation 2, decreased with the calcium content*

153

154

155

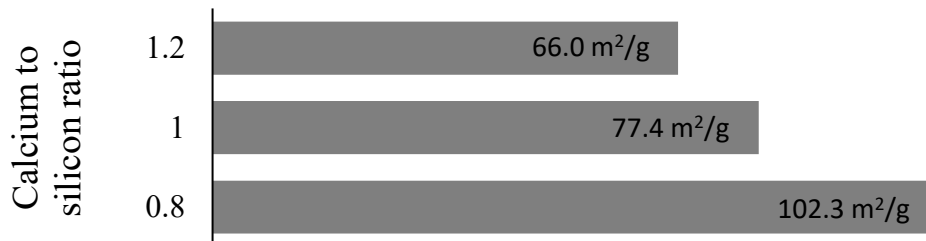
156

157

158

159

For crystal seeding applications, aside from mineralogy, the available surface area is also known to be a crucial factor. In the present study, it was examined through the determination of the specific surface area and the particle size distribution. The increase in specific surface area, which was determined by cryo-nitrogen adsorption and BET isotherms, was in good accordance with the increase of layer spacing detected in XRD. As a result, it is assumed that it does not represent the surface available for nucleation and growth, but mostly the inner surface of the hydrates, which were shown to share some characteristics with clay minerals [24] (Fig. 4).



160

161

162

*Fig. 4: Results of the cryo-nitrogen adsorption experiments. The specific surface area of calcium silicate hydrate with  $C/S = 1.2$  was reduced by ~30 %, as compared to  $C/S = 0.8$*

163

164

165

166

167

168

The particle size and distribution of micro- and nano-particles is strongly affected by the method of dispersion [25,26]. Experiments with varying dispersion times were conducted to give an estimate of the agglomeration effect, concerning the influence of the calcium to silicon ratio on particles size. Ultrasonic treatment reduced the mass median particle size to approximately 60 % of the original agglomerate size after one minute. No significant reduction in particle size was observed for longer dispersion times and re-agglomeration was observed for samples dispersed for longer than 5 minutes.

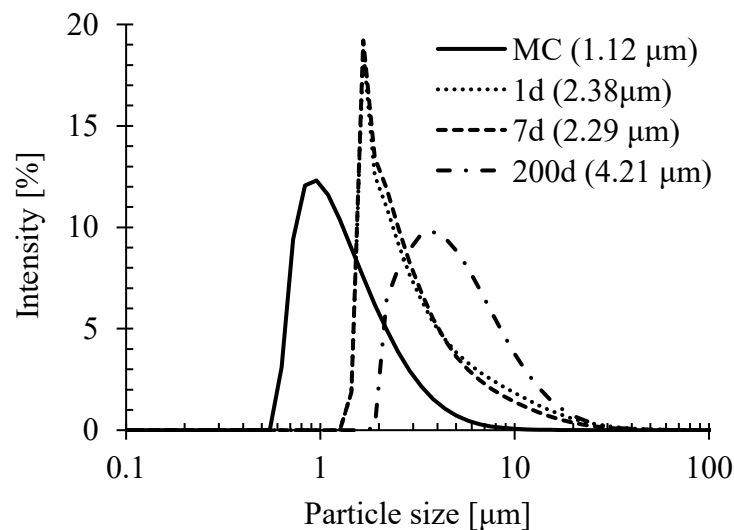
169 In the presence of sodium pyrophosphate as a stabilization agent, the particle size was slightly more  
 170 reduced with longer dispersion times, to 55 % of the original agglomerate size. Differences in the particle  
 171 sizes of samples with different C/S were observed for all preparation methods, before the samples were  
 172 treated with the ultrasonic rod. However, a trend caused by changes in the C/S was not evident (Tab. 1).  
 173 After dispersion, the differences were no longer significant. It is assumed that C-S-H forms relatively  
 174 loose bound aggregates during or after synthesis and that these aggregates can break down to a critical  
 175 size of a few micro-meters. At smaller sizes, a stabilization agent is necessary to prevent re-  
 176 agglomeration.

177 *Tab. 1: Mass median particle size, in  $\mu\text{m}$ , of unsuspended calcium silicate hydrates, prepared either under ambient conditions in a*  
 178 *shaker (AC) or mechanochemically (MC).*

C/S	0.8	1	1.2	1.4
AC Batch 1	1.88	3.65	2.99	2.02
AC Batch 2	1.30	1.11	0.59	1.31
MC	2.85	3.84	4.72	5.13

179 Different synthesis parameters were investigated to see whether C-S-H forms larger aggregates over  
 180 time. After seven days, no differences in agglomerate size were found, as compared to 1-day old C-S-  
 181 H. It was only after 200 days that bigger aggregates, with a mass median particle size of 4.2  $\mu\text{m}$ , were  
 182 formed. C-S-H prepared mechanochemically showed a smaller particle size, as compared to C-S-H  
 183 prepared under ambient conditions; most likely due to the higher shear conditions in the planetary ball  
 184 mill (Fig. 5).

185



186

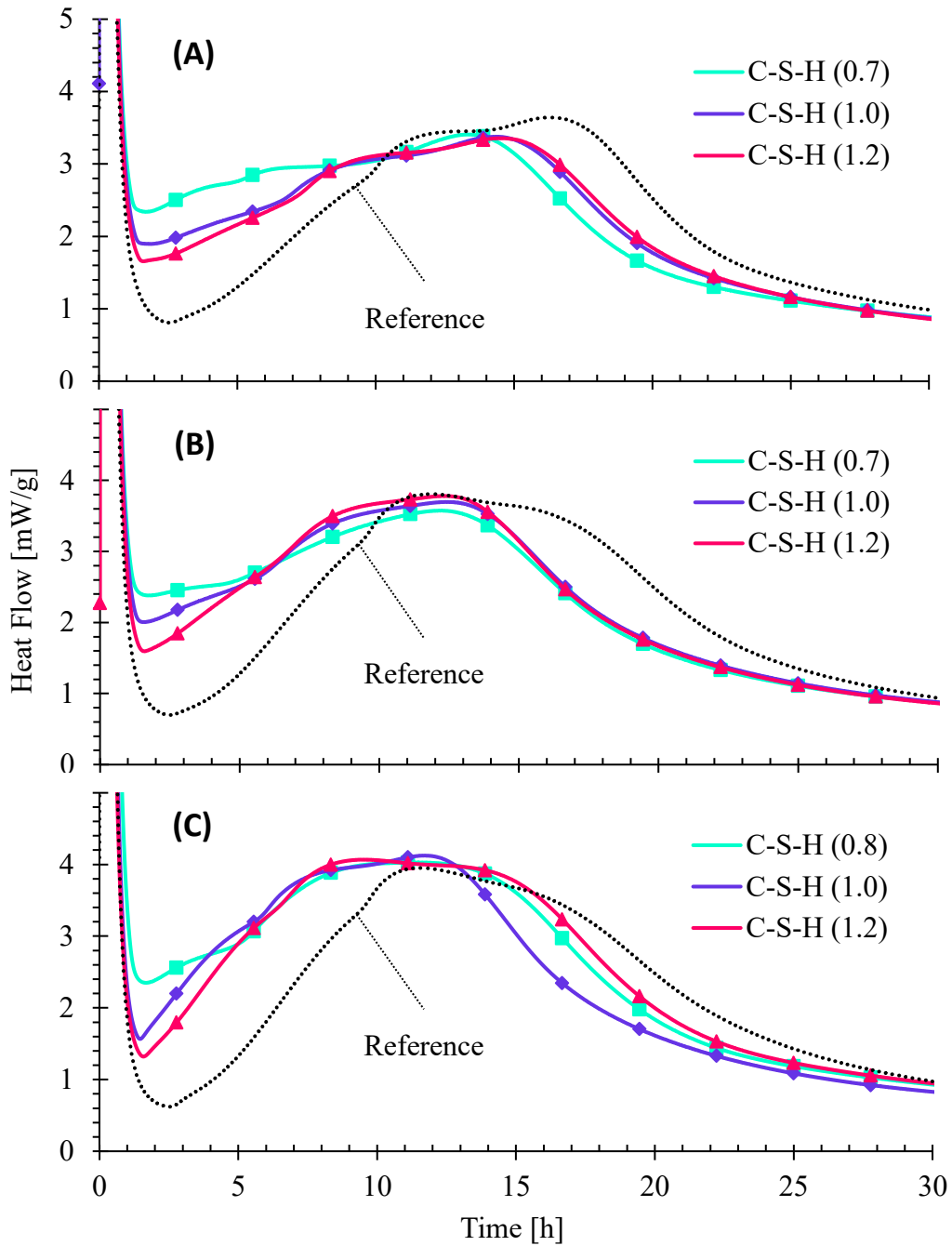
187 *Fig. 5: Particle size distribution of different calcium silicate hydrate suspensions dispersed for one minute. MC refers to*  
188 *mechanochemically prepared C-S-H. The other three samples were prepared under ambient conditions with different synthesis times. The*  
189 *mass median particle size is indicated in brackets.*

190 The results from particle size analysis were consistent with the results from XRD and BET, which  
191 suggests that it was mainly the inner surface which increased in size with rising silicon content.

## 192 5.2. *Influence of the calcium to silicon ratio on acceleration performance*

193 To evaluate the impact of stoichiometry, calcium silicate hydrates with C/S ratios between 0.7 and  
194 1.2 were applied, to accelerate the tricalcium silicate and cement pastes. The differences in the rheology  
195 of fresh pastes, the heat of hydration, the setting behaviour and strength development were monitored.

196 For isothermal heat flow calorimetry, the C-S-H was prepared either mechanochemically or by  
197 pozzolanic reaction under ambient conditions, to reveal the influence of different synthesis methods.  
198 Fig. 6 shows the impact of 1 wt.% C-S-H on cement hydration. All C-S-H additives accelerated heat  
199 development by approximately 3 h (determined by the peak hydration heat) and appeared to reduce the  
200 delay during the dormant period. The dormant period was significantly less pronounced with the  
201 addition of low calcium C-S-H. No differences in this trend, attributable to either the synthesis duration  
202 (not shown), the method or the cement fineness, were observed.



203

204

205

206

*Fig. 6: Impact of 1 wt.-% C-S-H, with varying stoichiometry, on the hydration of cement with different fineness A) CEM I 52.5R accelerated with C-S-H prepared under ambient conditions B) CEM I 42.5R accelerated with C-S-H prepared under ambient conditions C) CEM I 42.5R accelerated with C-S-H prepared mechanochemically*

207

208

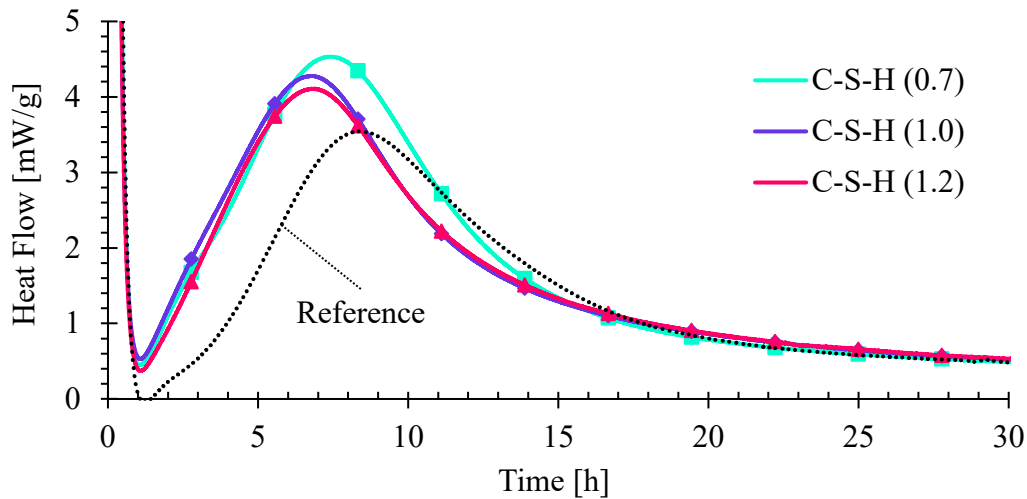
209

210

211

In 2009, Alizadeh et al. reported that synthetic semi-crystalline C-S-H might alter the C/S of the calcium silicates formed in C<sub>3</sub>S pastes during hydration. Furthermore, in 2018 Horgnies et al. confirmed the results of Seligmann et al.'s 1969 experiment, that crystalline C-S-H (afwillite) can induce the formation of crystalline hydration products, during the hydration of alite [11,27,28]. An investigation of the effects of C-S-H with varying stoichiometry, on C<sub>3</sub>S hydration, was therefore of special interest here.

212 While the stoichiometry of synthetic C-S-H mainly influenced the dormant period in cement hydration,  
213 in tricalcium silicate it was mainly the maximum heat flow which was altered, with the peak heat flow  
214 accelerating by approximately 2h. As with cement, low lime C-S-H had a slightly more pronounced  
215 effect, with the enhanced maximum shifting to later times, without a delay in the acceleration period  
216 (Fig. 7).



217

218 *Fig. 7: Impact of 1 wt.-% C-S-H, prepared mechanochemically with varying stoichiometry, on the hydration of triclinic tricalcium*  
219 *silicate paste*

220 To investigate whether there were any effects on the hydration products, the silicate polymerization  
221 of hydrating  $C_3S$  pastes were monitored with  $^{29}Si$  MAS-NMR. The accelerating effect of C-S-H was  
222 visible in the faster depletion of  $Q^0$  silicate species in seeded pastes. The effects of seeding appeared to  
223 be less pronounced after several days of hydration; the sample seeded with 1 wt.-% calcium silicate  
224 hydrate, with  $C/S = 1.2$ , actually already showed a negative effect after seven days (Fig. 8).

225

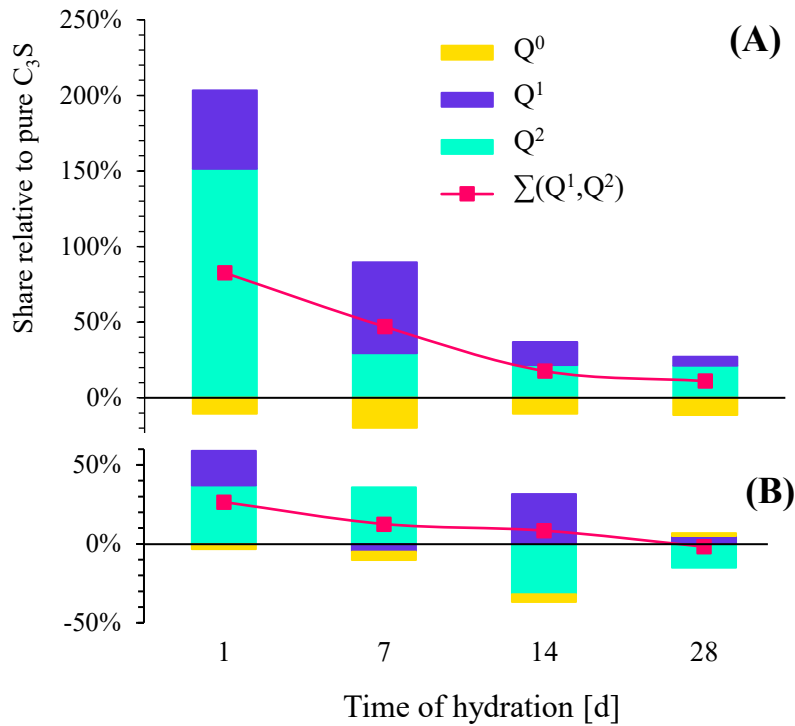


Fig. 8: Development of the silicate species in  $C_3S$  pastes seeded with 1 wt.-% C-S-H, relative to the phase development in pure  $C_3S$  A)

C/S = 0.8 B) C/S = 1.2

226

227

228

229

230

231

232

233

234

235

236

237

238

239

240

241

242

243

After one day of hydration, the mean chain length in  $C_3S$  seeded with C-S-H, was higher as compared to the reference sample, for both C/S ratios. Based on the data presented in Tab. 2, it seems that the silicate polymerization in  $C_3S$  increased to a maximum after several days of hydration and that it continued to decrease slowly until equilibrium was reached. It is assumed that a fully hydrated  $C_3S$  sample will show mostly dimeric C-S-H with a C/S of 1.7, due to excess calcium [23]. Additions of synthetic C-S-H accelerated the hydration reactions, as was additionally confirmed through TGA (Fig. 9). A possible consequence of this is that the peak polymerization was reached earlier for  $C_3S$  seeded with C/S = 0.8. Alizadeh et al. assumed that C-S-H seeds with a higher degree of silicate polymerization, also induce the formation of hydration products with a higher degree of silicate polymerization content. Our findings might give support to this theory, which would imply that the same would be valid for lower degrees of polymerization, as is characteristic for C-S-H with C/S = 1.2 ( $\overline{CL} = 2.32$ ). This was the case in seeded  $C_3S$  pastes with hydration times of more than 14 days; the mean chain length was slightly higher when seeded with  $C_{0.8n}S_nH_x$  and lower for  $C_{1.2n}S_nH_x$ , compared to the unseeded paste. Acceleration of the hydration processes without a change in the products cannot explain this effect solely, if one assumes that a shorter chain length is reached after more advanced hydration. Based on

244 the NMR and TGA data, the opposite was the case: hydration was delayed by  $C_{1.2n}S_nH_x$ , which caused  
 245 a lower degree of silicate polymerization and accelerated by  $C_{1.2n}S_nH_x$ , which caused a longer mean  
 246 chain length in the hydration products.

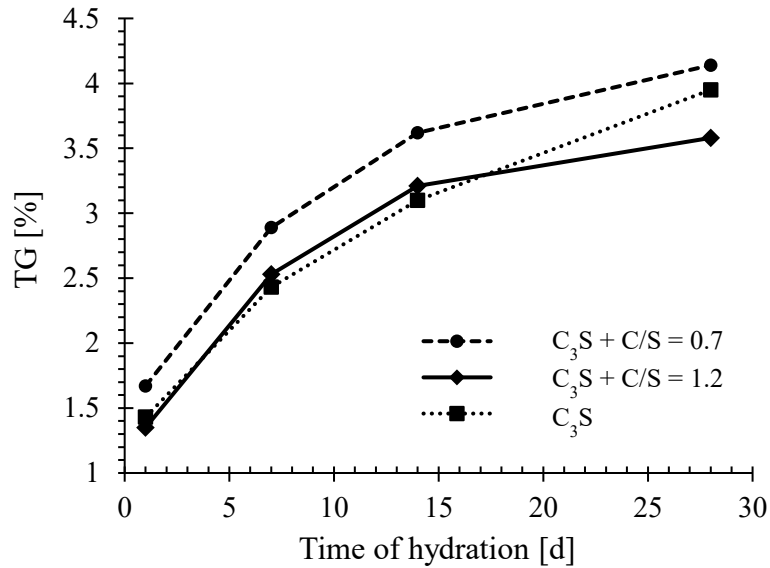
247 Direct evidence is difficult to gather, since C-S-H formed on  $C_3S$  grains or on seeds is barely  
 248 distinguishable by batch analysing methods. Currently, ongoing research is focusing on giving more  
 249 support to the question of whether C-S-H seeds alter hydration products based on their calcium to silicon  
 250 ratio.

251 *Tab. 2: Mean chain length of hydration products in pure and seeded  $C_3S$  paste, after 1, 7, 14 and 28 days of hydration, based on*  
 252 *quantitative  $^{28}Si$  MAS-NMR data and calculated according to equation (2)*

	Time of hydration [days]			
	1	7	14	28
$C_3S$	2.90	3.50	3.15	3.03
$C_3S + C_{0.8n}S_nH_x$	3.48	3.21	3.21	3.18
$C_3S + C_{1.2n}S_nH_x$	3.01	4.14	2.60	2.83

253

254 The less beneficial effect of high calcium, compared to low-calcium C-S-H seeds, in  $C_3S$  pastes was  
 255 confirmed by thermogravimetric analysis of the hydration products (Fig. 9). Besides the information  
 256 about the quantity of C-S-H, a higher weight loss in the range of 25-200 °C might also indicate the  
 257 formation of C-S-H with a lower calcium to silicon ratio, as it was shown that the water content is related  
 258 to the C/S ratio. A change in the water content, caused by a change in silicate polymerization, was  
 259 nevertheless found to be minor for calcium rich C-S-H ( $C/S = 1 - 1.7$ ; compare Fig. 2), with the results  
 260 being conclusive according to the reduction of  $Q^0$  in NMR.

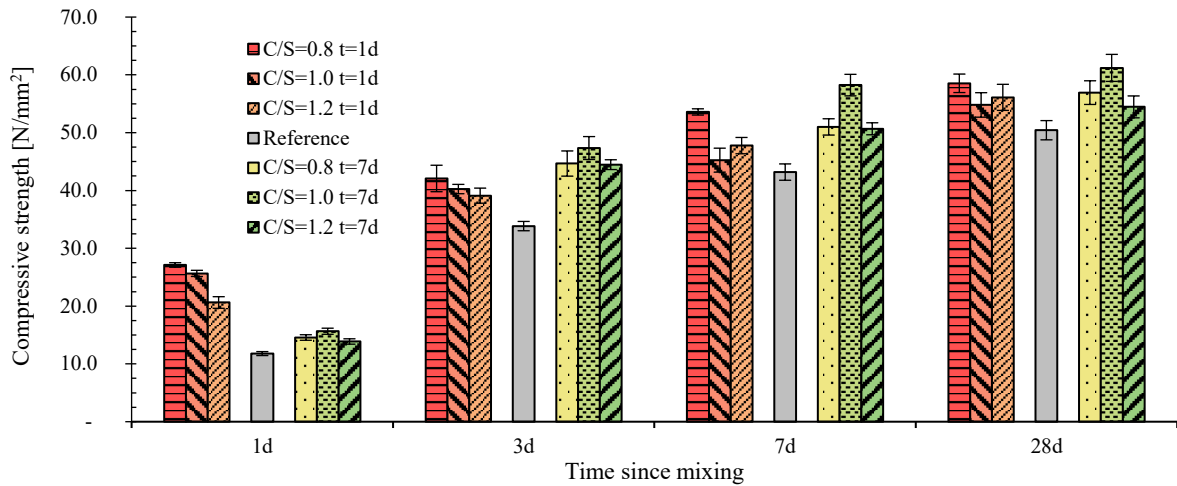


261

262 *Fig. 9: Confirmation of the observed beneficial effects of low-calcium C-S-H, by analysis of the weight loss between 100 and 250 °C*  
 263 *attributed to water from C-S-H phases. For comparison, the development of the silicate species of the hydration product is also shown.*

264 Based on the conclusive results from calorimetry and NMR, the same performance trend was  
 265 expected in strength development. Accordingly, C-S-H was prepared under ambient conditions and kept  
 266 under agitation for one or seven days. After one and three days of hardening, the expected trend of  
 267 calcium silicate hydrates with a low C/S showing better performance, was confirmed for one-day-old  
 268 calcium silicate hydrate. The trend for long-term strength was not as pronounced as for early strength,  
 269 but C-S-H with a C/S of 0.8 was still significantly more effective. Surprisingly, this was not the case for  
 270 calcium silicate hydrate seeds prepared over seven days; while the difference in compressive strength  
 271 after one day was minor, the development of long-term strength confirmed that C-S-H with C/S = 1.0  
 272 was slightly more effective than C/S = 0.8 or 1.2 (Fig. 10). Since the reason for the C/S induced change  
 273 in performance is still under investigation, it is difficult to explain why C-S-H (C/S = 1) surpasses the  
 274 effects of the other two C-S-H samples; one possibility is the different formation speed of the silicate  
 275 structure, which might still be changing after 24 hours, although quantitatively the reaction is complete  
 276 within 24 hours. The investigation of a calcium silicate hydrate aged for one year (not shown), revealed  
 277 that performance decreases after a certain ageing time, but surprisingly compressive strength was still  
 278 enhanced by 90% after one day and by 9% after 28 days, compared to the unseeded reference cement.  
 279 The decrease in acceleration was most likely due to the formation of larger aggregates; the mass median  
 280 particle size of the one-year-old C-S-H, after one minute of dispersion, was 4.2 μm.





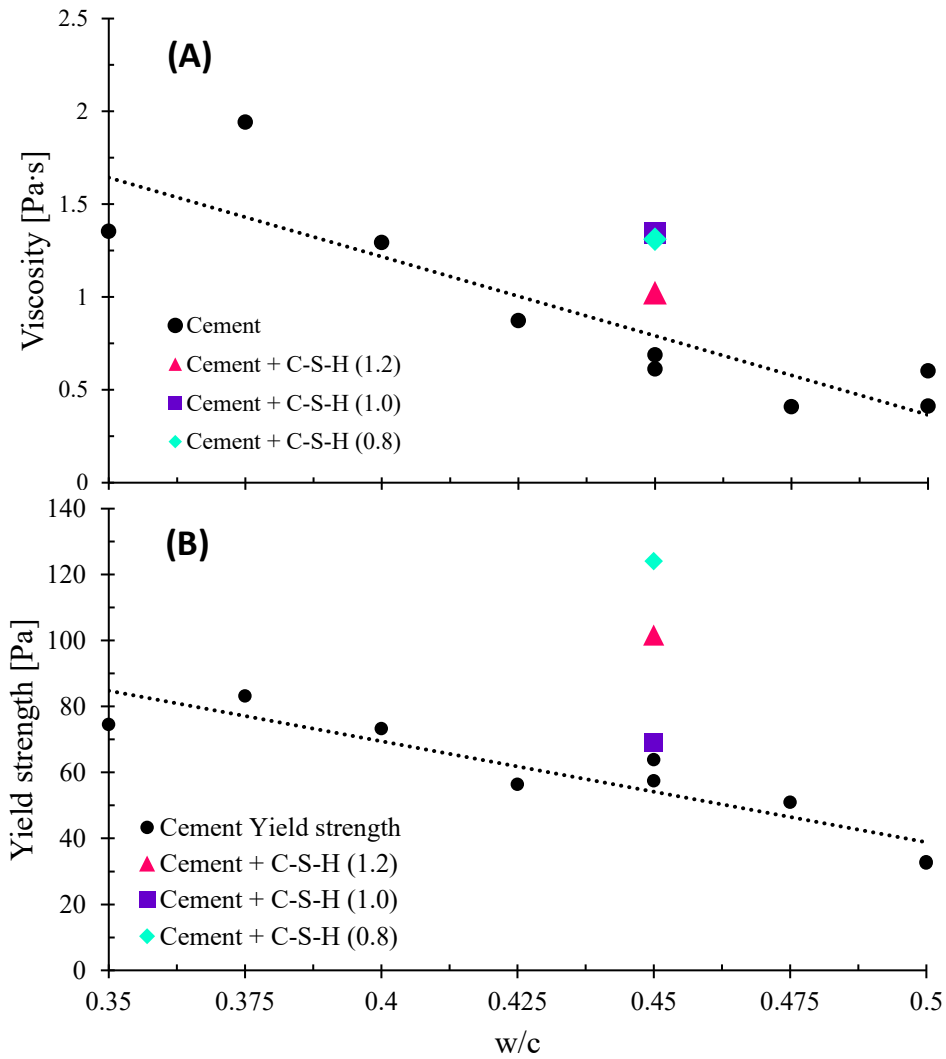
281

282 *Fig. 10: Compressive strength development of cement stone, depending on the stoichiometry and reaction time of the C-S-H. The left*  
 283 *block of each testing interval was prepared with 1 wt.-% one-day old C-S-H, the right block with seven-day old C-S-H. The reference*  
 284 *cement is in between, without a pattern.*

285 The acceleration of cements with different water to cement ratios was also tested (not shown) and it  
 286 was found that C-S-H compromises long-term strength when the water content is low but accelerates  
 287 early strength in all cases. This might be a result of the formation of a denser microstructure in seeded  
 288 cements, which hence restricts water mobility at older times.

289 Since synthetic calcium silicate hydrate appeared to mostly affect early strength development, the  
 290 setting behaviour of cement pastes with and without C-S-H was investigated with Vicat needle  
 291 penetration. Initial and final setting times were determined with tangents and confirmed expectations of  
 292 a significant impact, with low-calcium C-S-H being more effective, although the differences due to C/S  
 293 were minor.

294 During the preparation of specimens for compressive strength and Vicat testing, it was observed that  
 295 C-S-H enhances water demand. Rheological investigations confirmed that viscosity and yield strength  
 296 increased when C-S-H was applied. Fig. 11 illustrates these results in comparison with the results for  
 297 cement pastes with varying water to cement ratios, down to the limit of workability ( $w/c = 0.35$ ). In  
 298 relation to cement without additives, the increase in viscosity due to C-S-H was minor, although the  
 299 enhanced yield strength was nevertheless significant; a clear difference caused by C-S-H stoichiometry  
 300 was visible. As expected, the impact of low-calcium C-S-H was major but surprisingly, the impact of  
 301 high-calcium C-S-H was lower than for  $C/S = 1$ .



303

304 *Fig. 11: Impact of C-S-H on the rheological properties of cement paste with a water to cement ratio of 0.45. A) Impact on yield strength*  
 305 *B) Impact on plastic viscosity*

306 As was described earlier, the water content of C-S-H changes with the calcium to silicon ratio, with  
 307 the water content of C-S-H being sensitive to drying. It is possible that when dispersed in water, C-S-H  
 308 rehydrates its interlayer spaces to a certain degree and hence reduces the free water available for  
 309 hydration. The intent of the investigations shown in Fig 12 was to prove that rheological changes cannot  
 310 be explained solely through possibly reduced free water.

311 **6. Summary and Conclusion**

312 Several physical and chemical properties of synthetic calcium silicate hydrates were found to change  
 313 according to their initial stoichiometry. With rising calcium content, the mean silicate chain length

314 decreased, which was visible in the decreasing  $Q^2$  signal in NMR and the related reflex in XRD. The  
315 basal spacing decreased, which was found to be related to the reduced interlayer water content;  
316 consequently, the specific surface area decreased. These findings correlate well with literature data.

317 Synthetic calcium silicates accelerated the hydration of all cementitious materials and it was found  
318 that they altered the rheology of fresh pastes significantly. In compressive strength tests of pastes  
319 prepared with decreasing water contents, it was found that C-S-H compromised long-term strength in  
320 low w/c samples. It is assumed that this adverse effect was the result of a water deficiency, caused either  
321 by the drastically elevated water demand resulting from the large surface area of the C-S-H, or by the  
322 formation of a dense microstructure which would result from the C-S-H seeding mechanism proposed,  
323 thus restricting the mobility of water in the specimens. Whether C-S-H exerts such a drastic impact on  
324 cement microstructure is the focus of ongoing investigations.

325 Based on the trends in the characteristics of the C-S-H prepared, it was expected that the performance  
326 in accelerating cement hydration would show a similar trend and that either low-calcium or high-calcium  
327 C-S-H would be superior. In calorimetry, compressive strength, setting time, ultra-sonic sound speed,  
328 NMR and TGA experiments with hydrating cement or tricalcium silicate paste, it was confirmed that C-  
329 S-H with  $C/S = 0.8$  accelerates cement hydration more than C-S-H with  $C/S = 1.2$ . This confirms  
330 Alizadeh et al's findings, while contradicting those of Land et al, that calcium-rich C-S-H seeds are  
331 more effective.

332 Specimens with equimolar ratios showed behaviour deviating from expectations in rheology and  
333 compressive strength tests (C-S-H aged for 7 days), which indicates that more than one property of C-  
334 S-H is relevant for performance, while highlighting the importance of systematic investigation. As was  
335 shown in this study and as is known in the literature, C-S-H does not show a continuous change in  
336 properties over the complete range of  $C/S = 0.7$  to  $1.45$ , where it is usually referred to as C-S-H I. The  
337 discontinuity occurred approximately at  $C/S = 1.0$  and might explain why seeding with  $C_nS_nH_x$  deviated  
338 from expectations [29].

339 Further work will be dedicated to finding direct evidence and more support for the theory that seeding  
340 results in the formation of altered hydration products. The preparation, characterization and application  
341 of crystalline C-S-H phases is therefore part of ongoing work giving promising insights to surface

342 effects. Additionally, more focus will be placed on the impact of C-S-H on the pore solution, since its  
343 enormous specific surface area shows potential for adsorption processes that might create local gradients  
344 in ion consternation.

## 345 **7. Conflict of interests**

346 The authors declare that there is no conflict of interest.

## 347 **8. Acknowledgement**

348 This research was supported by the Deutsche Forschungsgemeinschaft, DFG, project number STE  
349 1086/15-1.

## 350 **9. References**

- 351 [1] M.S. Shetty, Concrete technology: Theory and practice, 7th ed., S. Chand & Company PVT. Ltd.,  
352 1982.
- 353 [2] P. Domone, J. Illston, Construction Materials: Their Nature and Behaviour, Fourth Edition, CRC  
354 Press, 2010.
- 355 [3] H.F.W. Taylor, Proposed Structure for Calcium Silicate Hydrate Gel, J American Ceramic  
356 Society 69 (1986) 464–467.
- 357 [4] E. Bonaccorsi, S. Merlino, H.F.W. Taylor, The crystal structure of jennite,  
358  $\text{Ca}_9\text{Si}_6\text{O}_{18}(\text{OH})_6 \cdot 8\text{H}_2\text{O}$ , Cement and Concrete Research 34 (2004) 1481–1488.
- 359 [5] J.J. Chen, L. Sorelli, M. Vandamme, F.-J. Ulm, G. Chanvillard, A Coupled  
360 Nanoindentation/SEM-EDS Study on Low Water/Cement Ratio Portland Cement Paste:  
361 Evidence for C-S-H/ $\text{Ca}(\text{OH})_2$  Nanocomposites, J American Ceramic Society (2010) 577.
- 362 [6] S. Grangeon, A. Fernandez-Martinez, A. Baronnet, N. Marty, A. Poulain, E. Elkaïm, C. Roosz, S.  
363 Gaboreau, P. Henocq, F. Claret, Quantitative X-ray pair distribution function analysis of  
364 nanocrystalline calcium silicate hydrates: A contribution to the understanding of cement  
365 chemistry, Journal of applied crystallography, 50 (2017) 14–21.

- 366 [7] P. Juilland, L. Nicoleau, R.S. Arvidson, E. Gallucci, Advances in dissolution understanding and  
367 their implications for cement hydration, RILEM Tech Lett 2 (2017) 90.
- 368 [8] G. Land, D. Stephan, Controlling Cement Hydration with Nanoparticles, Cement and Concrete  
369 Composites 57 (2015) 64–67.
- 370 [9] L. Nicoleau, Accelerated growth of calcium silicate hydrates: Experiments and simulations,  
371 Cement and Concrete Research 41 (2011) 1339–1348.
- 372 [10] S. Thomas, Der Wirkmechanismus von X-Seed - Crystal Speed Hardening, BASF Product  
373 Presentation (2009) 1–13.
- 374 [11] R. Alizadeh, L. Raki, J.M. Makar, J.J. Beaudoin, I. Moudrakovski, Hydration of Tricalcium  
375 Silicate in the Presence of synthetic Calcium–Silicate–Hydrate, Journal of Materials Chemistry  
376 19 (2009) 7937.
- 377 [12] J. Sun, H. Shi, B. Qian, Z. Xu, W. Li, X. Shen, Effects of synthetic C-S-H/PCE nanocomposites  
378 on early cement hydration, Construction and Building Materials 140 (2017) 282–292.
- 379 [13] A. Picker, L. Nicoleau, A. Nonat, C. Labbez, H. Cölfen, Identification of binding peptides on  
380 calcium silicate hydrate: A novel view on cement additives, Advanced materials (Deerfield  
381 Beach, Fla.) 26 (2014) 1135–1140.
- 382 [14] F. Pelisser, P.J.P. Gleize, A. Mikowski, Effect of poly(diallyldimethylammonium chloride) on  
383 nanostructure and mechanical properties of calcium silicate hydrate, Materials Science and  
384 Engineering A (2010) 7045–7049.
- 385 [15] J.J. Beaudoin, L. Raki, R. Alizadeh, A 29Si MAS NMR study of modified C–S–H  
386 nanostructures, Cem Concr Comp 31 (2009) 585–590.
- 387 [16] A. Franceschini, S. Abramson, V. Mancini, B. Bresson, C. Chassenieux, N. Lequeux, New  
388 covalent bonded polymer–calcium silicate hydrate composites, J. Mater. Chem. 17 (2007) 913–  
389 922.
- 390 [17] G. Land, D. Stephan, The effect of synthesis conditions on the efficiency of C-S-H seeds to  
391 accelerate cement hydration, Cement and Concrete Composites 87 (2018) 73–78.

- 392 [18] G. Land, D. Stephan, The Synthesis of C-S-H Seeds Methods, Variables and their Impact on the  
393 Ability to accelerate Cement Hydration, ICCC, 2015.
- 394 [19] L. Nicoleau, The Acceleration of Cement Hydration by Seeding: Influence of the Cement  
395 Mineralogy, Ibautil (2012).
- 396 [20] K. Xian-ming, J. Ling-fei, Influences of nano-sized C-S-H Particles on Cement Hydration of  
397 OPC in the Presence of Fly Ash or Polycarboxylate Superplasticizer, ICCC, 2015.
- 398 [21] K. Garbev, Struktur, Eigenschaften und quantitative Rietfeldanalyse von hydrothermal  
399 kristallisierten Calciumsilikathydraten (C-S-H Phasen), Wissenschaftliche Berichte des  
400 Forschungszentrum Karlsruhe in der Helmholtz-Gemeinschaft FZKA 6877 (2004) 1–271.
- 401 [22] F. Saito, Mechanochemical synthesis of hydrated calcium silicates by room temperature grinding,  
402 Solid State Ionics 101-103 (1997) 37–43.
- 403 [23] B. Lothenbach, A. Nonat, Calcium silicate hydrates: Solid and liquid phase composition, Cement  
404 and Concrete Research 78 (2015) 57–70.
- 405 [24] J.J. Beaudoin, H. Dramé, L. Raki, R. Alizadeh, Formation and characterization of calcium silicate  
406 hydrate–hexadecyltrimethylammonium nanostructure, J. Mater. Res. 23 (2008) 2804–2815.
- 407 [25] P. Sikora, A. Augustyniak, K. Cendrowski, P. Nawrotek, E. Mijowska, Antimicrobial Activity of  
408 Al<sub>2</sub>O<sub>3</sub>, CuO, Fe<sub>3</sub>O<sub>4</sub>, and ZnO Nanoparticles in Scope of Their Further Application in Cement-  
409 Based Building Materials, Nanomaterials (Basel, Switzerland) 8 (2018).
- 410 [26] N. Hamed, M.S. El-Feky, M. Kohail, E.-S.A.R. Nasr, Effect of nano-clay de-agglomeration on  
411 mechanical properties of concrete, Construction and Building Materials 205 (2019) 245–256.
- 412 [27] M. Horgnies, L. Fei, R. Arroyo, J.J. Chen, E.M. Gartner, The effects of seeding C<sub>3</sub>S pastes with  
413 afwillite, Cement and Concrete Research 89 (2016) 145–157.
- 414 [28] Paul Seligmann, Nathan R. Greening, Phase Equilibria of Cement-Water, Proceedings of the  
415 National Academy of Sciences (Tokio) (1969) 179–2002.
- 416 [29] A. Nonat, The structure and stoichiometry of C-S-H, Cement and Concrete Research 34 (2004)  
417 1521–1528.
- 418

